UiO : Department of Physics
University of Oslo

Approximating the ${}^1S_0$ Partial Wave of Nucleon-Nucleon Scattering With Effective Field Theory

Erlend Lima

April 12, 2021

Abstract

Basic effective field theory is presented and used to derive nuclear toy potentials for np-scattering of ${}^1S_0$ partial waves. The Reid68 potential is used to fit the potentials in the $10^{-3} - 10^{-1}$ MeV lab energy range, and compared in the $10^{-3} - 10^{2}$ MeV range. Other regions of fit were explored, confirming that the more infrared region, the better, but the aforementioned ranges were chosen to agree with Lepage. The fitting procedure was met with several difficulties, leading to poor fits and time consuming computations. Different values of the cutoff parameter Λ were explored, but no systematic power-law improvement improvement was seen as would be expected by chiral power counting. The closest improvements was found for $\Lambda = 100$ MeV for pionless potentials and $\Lambda = 150$ MeV when including 1π term. The cause of this discrepancy was not identified and remains unresolved. The pionless potentials LO and NNLO obtained their minima below $\Lambda = m_\pi$, indicating that the inclusion of pions is necessary to model higher energy physics. Including a one pion exchange toy potential based on the largest Yukawa term in the Reid68 potential indeed increased the optimal value of Λ to about 270 MeV, in accordance with the results of Lepage.

GitHub repository: https://github.com/ErlendLima/NuclearForces

Contents

1 Introduction

> [It was] a whole new world. It was as if, suddenly, we had broken into a walled orchard, where protected trees flourished and all kinds of exotic fruits had ripened in great profusion.
>
> *Cecil F. Powell*
> *on the discovery of the pion[1]*

1.1 Early Models on the Nuclear Force

The onset of quantum theory in the 1920s laid the foundation for understanding the interactions between nucleons from first principles. There were difficulties in explaining how the nucleus kept together under the repulsion between the protons, and in developing a formalism to understand the nucleus. A breakthrough came in 1935 when Hideki Yukawa proposed his meson theory, where he used then-modern field calculations to predict the existence of mesons[2]. He proposed an attractive force between the nucleons mediated by mesons, stemming from the residual strong force of the underlying quark structure[1]. The success of Yukawa theory was solidified by the later discovery of the π-meson[3] and heavier (ρ, ω, ...) mesons[4].

Later work on pion theories in the 1950s had modest success with explaining nucleon-nucleon (NN) scattering and properties of the deuteron involving one-pion exchange, while multiple-pion exchange failed to produce reasonable results[5, 6, p. 4]. The discovery of heavier mesons during the 1960s motivated one boson exchange models (OBE), models that still are of use today. There were a plethora of nucleon potentials developed on these ideas (Stony Brook[7], Paris[8], Bonn[6]), and the nucleon force problem appeared to have been satisfyingly solved.

Alas, the development of quantum chromo-dynamics (QCD) in 1970s revealed that the mesons themselves could be derived from more fundamental principles, and the work on establishing the theoretical framework for nuclear interactions from first principles started all over again. Taking the low energy limit of QCD and exploiting chiral symmetry lead to chiral perturbation theory (ChPT), an effective field theory which has achieved unprecedented accuracy in modeling low energy nuclear potentials.

1.2 Overview

The goal of this text is to calculate the phase shift of ${}^1S_0$ partial waves of np-scattering using potentials inspired by ChPT. The potentials are fitted to low energy phase shifts of the Reid68 potential and compared to its high energy phase shifts.

We will begin with a rudimentary exposition of ChPT and present the nuclear potentials that we will examine: LO, NLO and NNLO. Their form is sightly changed by only including a one-pion exchange term modeled after the heaviest Yukawa term of the Reid68 potential, thereby being simpler than the proper ChPT potentials. In the methods section their

[1] This is a modern interpretation as Yukawa's paper was more focused on applying field theory to compute the mass of the meson(s).

numerical implementation are presented, and a fitting procedure is developed to fit the potentials to low energy phase shifts. This turns out to be a tricky affair, requiring some care. Finally, phase shifts are computed for larger energies and compared to the "true" phase shifts from Reid68 and results of Lepage.

2 Theory

2.1 Quantum Chromo-Dynamics

Quantum chromo-dynamics is the base on which our modern understanding of the nuclear force stands, but it cannot itself be used to model the nuclear force by any practical means. This is due to its unperturbative nature at low energies, the energy regime of nuclear interactions. The problem remained intractable until Weinberg in 1979 developed the concept of effective field theories (EFT)[9].

The underlying idea of EFT is reminiscent of multipole expansion in electromagnetic field theory. The complex short-range interactions of an electromagnetic field can be approximated by a simpler structure when one is only concerned about the long range interaction, such as treating an arbitrary charge distribution as a point charge at large distances. Perhaps the most advantageous property of an EFT is that a bound on the resulting approximation error can be systematically established and improved, akin to including more multipoles and computing the order of the truncation.

Chiral perturbation theory (ChPT) is an EFT of QCD built upon the symmetries relevant in the nuclear energy regime allowing for a systematic treatment of the model errors. Instead of having quarks and gluons as the degrees of freedom as they are in QFT, the effective degrees of freedom become the nucleons and pions. More energetic phenomena like nuclear resonances and mesons are integrated out[10, p. 11]. This leads to ChPT's inability to model such phenomena, and might be taken as an argument against it. However, the model's inability to account for higher energy interactions does not invariably lead to failure to explain low energy interactions. As argued by Ken Wilson, it is better to admit that the high energy physics are unknown and treat it as such. Since there are many high energy extensions consistent with a low energy model, there is no need to pick the most "realistic" model, only the most practical.

There are several ways to develop an EFT for the nuclear regime. The majority of modern nuclear EFTs are based on chiral symmetry, using the approach outlined by Weinberg in 1979 and expanded upon in 1990[11]. The Lagrangian used is the most general possible while being constrained by chiral and additional symmetries[2]. From the resulting infinite amount of terms, a finite number is selected through perturbative expansion. The details are technically complicated and surprisingly unenlightening. Only a short high level overview will be given in the following paragraphs. More details are available in a plethora of write-ups, such as [10, 12, 13].

To perform a perturbative expansion it is necessary to identify separation of scales. For ChPT there are two scales: a soft scale Q being the external momenta or the pion mass $m_\pi \approx 140\,\text{MeV}$, and a hard scale[3] $\Lambda_\chi \sim 1\,\text{GeV}$, also called the symmetry breaking scale or hadronic scale. The expansion is performed in powers of $\left(Q/\Lambda_\chi\right)^\nu$, where ν is known as the *chiral order*.

[2] The curious reader might wonder why chiral symmetry has such a central role in nuclear low energy phenomena. As far as I know, besides the normal QCD arguments of symmetries and Goldstone bosons, there is no intuitive explanation for the connection between chirality and nuclear interactions.

[3] The value of the hard scale Λ_χ is unknown, but is bounded above by $4\pi F_\pi \approx 1200\,\text{MeV}$[10, p. 18] and below by the first non-Goldstone meson ρ, $m_\rho \approx 770\,\text{MeV}$. Picking a value in the range $500 - 1000$ MeV is a common choice for calculations[13, p. 29]. Others suggest going so low as 300 MeV[14, 13, p. 64, p. 36].

The ChPT Lagrangian can be separated into terms for different interactions,

$$\mathcal{L}_{\text{eff}} = \mathcal{L}_{\pi\pi} + \mathcal{L}_{\pi N} + \mathcal{L}_{NN} + \dots,$$

where $\mathcal{L}_{\pi\pi}$ is pionic dynamics, $\mathcal{L}_{\pi N}$ is interactions between pions and a nucleon, and $\mathcal{L}_{NN}$ the contact[4] interactions between two nucleons. The ellipsis denotes higher order interactions, such as the interaction of pions and two nucleons $\mathcal{L}_{\pi NN}$. Each of these terms contains in turn an infinite amount of terms. The choice of which terms to include in our effective theory is done through a rather technical scheme whereby one assigns a chiral order to all associated Feynman diagrams and selects a highest order $\nu \geq 0$. The number of terms associated with a particular ν is guaranteed to be finite, and the error from ignoring all higher order diagrams is bounded by $\left(Q/\Lambda_\chi\right)^{\nu+1}$.

From $\nu = 0$ we obtain the lowest, or leading, order (LO). It is rather crude with only two NN contact terms, but already accounts for the tensor force, necessary to describe the deuteron[15, p. 18]. Partial waves of very high angular momentum are adequately described, while S-waves are only roughly correct up to medium range. $\nu = 1$ vanishes, meaning the next-to-leading order (NLO) has $\nu = 2$. This order includes central, spin-spin, spin-orbit and tensor terms; all spin-isospin structures necessary to describe the two-nucleon force phenomenologically. The intermediate-range interaction is not yet well described. It is known[6, 8] that $\Delta(1232)$-isobar contributions are necessary for a good description of the nuclear force, and these are introduced in $\nu = 3$, the next-to-next-to-leading order (NNLO). $\nu = 4$ (N^3LO) is currently the highest order which is computationally feasible, but is not of interest to us here due to its complexity.

There is undoubtedly a lot of work involved in creating an EFT potential. Is this really necessary, one may wonder, why not use a phenomenological potential instead? It is important to realize that EFT is not glorified curve fitting. When a term is added to a phenomenologically motivated potential trying to account for some high energy discrepancy, high energy data is required to improve the fit, and the majority of the improvement will lie at high energies. In contrast, adding a higher order term to an EFT potential gives a better fit for all energies, and requires only low energy data to perform the fit. It is a method guaranteed to systematically improve the solution, where loss of improvement hints at as of yet unknown physics.

2.2 The EFT Potentials

After the brief overview of how to derive nuclear potentials from EFT, it is time to present the results. The general form of the LO, NLO and NNLO potentials is[15, p. 30-36].

$$V^{LO} = V_{\text{ct}}^{(0)} + V_{1\pi} \tag{2.1}$$

$$V^{NLO} = V_{LO} + V_{\text{ct}}^{(2)} + V_{2\pi}^{(2)} \tag{2.2}$$

$$V^{NNLO} = V_{NLO} + V_{2\pi}^{(3)}, \tag{2.3}$$

where $V_{\text{ct}}^{(n)}$ denotes contact terms of chiral order n, and $V_{k\pi}^{(m)}$ denotes k-pion exchange terms with chiral order m. The greyed-out pion exchange terms are excluded in our toy potentials.

[4] An interaction modeled by having no force carrier is a *contact* interaction, having a special place due to its mathematical simplicity.

The contact terms are long and terribly unexciting. For the partial wave ${}^1S_0$ they reduce to simply

$$V^{LO}_{ct,{}^1S_0}(p,q) = C_0 \tag{2.4}$$
$$V^{NLO}_{ct,{}^1S_0}(p,q) = C_2(p^2+q^2) \tag{2.5}$$
$$V^{NNLO}_{ct,{}^1S_0}(p,q) = C_4(p^4+q^4) + C_4' p^2 q^2. \tag{2.6}$$

The coefficients C_0, C_2, C_4, C_4' are the model parameters or *low energy coefficients* (LECs). There exists theoretical values for the coefficients, but due the truncation and the ensuing renormalization, the values are rather useless. They are instead obtained by fitting to data.

The full one-pion exchange term has the form

$$V_{1\pi}(\vec{p},\vec{p}\,') = -\frac{g_A^2}{4f_\pi^2}\boldsymbol{\tau}_1\cdot\boldsymbol{\tau}_2\frac{\vec{\sigma}_1\cdot\vec{q}\vec{\sigma}_2\cdot\vec{q}}{q^2+m_\pi^2},$$

or in position space[13, p. 30]:

$$V_{1\pi}(r) = \alpha_\pi\boldsymbol{\tau}\cdot\boldsymbol{\tau}\frac{\boldsymbol{\sigma}_1\cdot\boldsymbol{\nabla}\boldsymbol{\sigma}_2\cdot\boldsymbol{\nabla}}{m_\pi^2}v_\mu(r), \tag{2.7}$$

We, however, will be using a much simpler interaction: a Yukawa potential. This is motivated by the fact that the radial part of (2.7) approaches the Yukawa potential as the distance becomes large:

$$v_\mu(r) \xrightarrow[r\to\infty]{} V_{\text{Yukawa}}(r) = -C_\mu^2\frac{\exp(-\eta\mu r)}{r},$$

where μ is the meson mass, C_μ the coupling constant and η some exponent. The Hankel transform of the potential transforms to the potential basis, yielding

$$V_{\text{Yukawa}}(p,q) = \frac{C_\mu}{4\mu pq}\ln\left[\frac{(\mu\eta)^2+(p+q)^2}{(\mu\eta)^2+(p-q)^2}\right].$$

The *Reid68* potential is the sum of three Yukawa potentials, see description at subsection 2.4. As EFT allows for better description at lower energies, or equivalently larger distances, the long range term of the *Reid68* potential is chosen as one-pion exchange interaction with $\eta = 1$:

$$V_\pi(p,q) = \frac{C_\pi}{4m_\pi pq}\ln\left[\frac{m_\pi^2+(p+q)^2}{m_\pi^2+(p-q)^2}\right]. \tag{2.8}$$

The coupling coefficient C_π is not the same as the one set by Reid, instead being fit to data.

2.3 Regularization

A quirk of field theory is the need for renormalization and regularization. Loop diagrams corresponding with virtual particles cause ultraviolet divergence, i.e. gives rise to infinities

when integrating over all momenta. The solution is to regularize, whereby the infinities are removed through the introduction of a parameter Λ and a regularization scheme. Having subdued the divergences, the theory can be made independent on Λ through renormalization.

In theoretical calculations, the dimensional regularization scheme is a popular choice[13, p .41]. It preserves the underlying symmetries and allows for a simple power counting[16, p .5]. In addition it ensures that all virtual momenta are of the order of the soft scale, causing automatic renormalization. Alas, it is not suited for for numerical calculations[16], where instead cut-off regularization methods reign supreme. These methods introduce a cutoff-momentum Λ, removing all larger momenta. Unlike dimensional regularization, different values of Λ will change the values of the LECs. There are many different cutoff schemes, from a simple cutoff to highly intricate methods to balance different types of diagrams. Here we will use a simple Gaussian cutoff in momentum space:

$$V(p,q) \xrightarrow[\text{regularize}]{} f_\Lambda(p) V(p,q) f_\Lambda(q),$$

where

$$f_\Lambda(p) = \exp\left(-p^4/\Lambda^4\right).$$

The value of Λ is not given by theory, instead requiring educated guesswork and observing the behavior of the computed observables. Setting the cutoff too low will exclude too much high momentum physics, leading to a theory with low predictive power. Setting the cutoff too high will include high energy physics not accounted for by the EFT, allowing for divergences to crop up, again giving useless results. As a rule of thumb the value is set in the order of magnitude of the hard scale, $\Lambda \approx \Lambda_\chi$[10, p .41].

2.4 The Reid Potential

A specific instance of a generalized Yukawa potential is the *Reid potential*[17]. It was an incremental improvement on already existing potentials at that time, building a parameterized potential where the exponent in each term reflects some phenomenological properties of the nuclear force while the constants are fit to phase shift data without consideration for their physical interpretation. In the case of proton-neutron scattering, the potential for the partial wave ${}^1S_0$ consists of the three terms:

$$V(r) = V_a \frac{e^{-ax}}{x} + V_b \frac{e^{-bx}}{x} + V_c \frac{e^{-cx}}{x}$$

where $x = \mu r$, $\mu = 0.7$ MeV, $V_a = -10.463$ MeV, $V_b = -1650.6$ MeV, $V_c = 6484.3$ MeV, and $a = 1$, $b = 4$ and $c = 7$.

The individual terms are plotted in Fig. 2.1 along with their sum. Its construction becomes apparent, where the three terms interact to form a strongly repulsive potential at close range along with an attractive well at a distance of about 1 fermi.

The Reid potential for np ${}^1S_0$ was fit to several hundred data points of the phase shift in the region $0 - 350$ MeV, and thus should provide a good fit in this region[17].

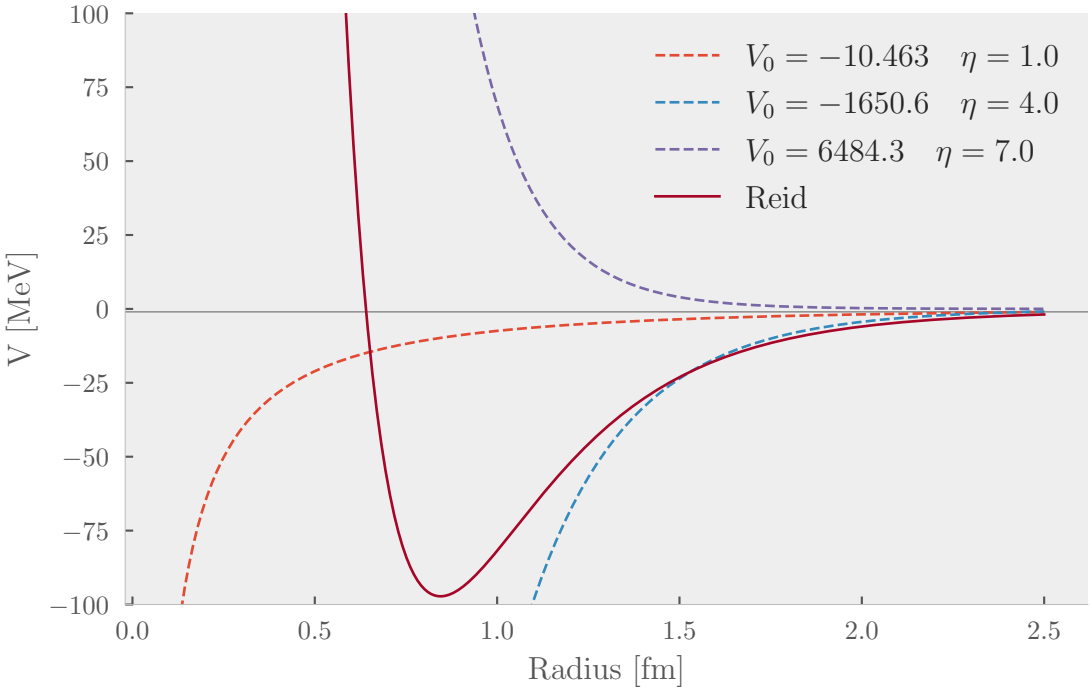

Figure 2.1: *The Reid potential (full stroke), a sum of three Yukawa potentials (dashed). It is has the typical characteristics of a nuclear force model, with a short range attractive potential followed by a repulsive core.*

2.5 Fitting to Data

The potential derived from EFT is incomplete, lacking values for its LECs that must be obtained from comparison to experimental data. The potential itself is unobservable [5] - instead one must use it to compute some other observable quantities. There are no hard and fast rules for which observables to use, common options being the scattering length and energy levels. Here we will for simplicity's sake only use the ${}^1S_0$ phase shift, at the cost of accuracy and fitting robustness.

[5] In fact, there is no reason to expect the EFT potential to converge to the "true" potential at all. EFT approximates the true high energy behavior by a simpler structure, reflected in the long range part of the EFT potential converging to the "true" potential while the short range part may deviate[13, p. 17]

Listing 1 Implementation of the EFT potentials.

```
#= EFT Potentials =#
#= Lowest leading order pionless EFT potential =#
struct LO <: Potential
    C₀::Float64
end

function (V::LO)(k, k′)
    V.C₀
end

#= Next-to-leading order pionless EFT potential =#
struct NLO <: Potential
    C₀::Float64
    C₂::Float64
end

function (V::NLO)(k, k′)
    V.C₀ + V.C₂*(k^2 + k′^2)
end

#= Next-to-next-to-leading order pionless EFT potential =#
struct NNLO <: Potential
    C₀::Float64
    C₂::Float64
    C₄::Float64
    C₄′::Float64
end
NNLO(c0, c2, c4) = NNLO(c0, c2, c4, c4)

function (V::NNLO)(k, k′)
    V.C₀ + V.C₂*(k^2 + k′^2) + V.C₄*(k^4 + k′^4) + V.C₄′*k^2*k′^2
end
function (V::NNLO)(k, k′)
    V.C₀ + V.C₂*(k^2 + k′^2) + V.C₄*(k^4 + k′^4) + V.C₄*k^2*k′^2
end


#= Pion interaction =#
struct Pion <: Potential
    mπ::Float64
    Vπ::Float64
end
Pion(Vπ::Real) = Pion(0.7, Vπ)

function (V::Pion)(k, k′)
    mπ = V.mπ
    V.Vπ/(4mπ * k*k′) * log((mπ^2 + (k+k′)^2)/(mπ^2 + (k-k′)^2))
end
```

3 Method

3.1 Code Implementation

Extending the previous Scattering.jl library to handle the potentials spawned by effective field theory is a simple matter. Each potential corresponds to a struct with the necessary coefficients, along with a callable method for evaluating the potential. These are shown in Listing 1.

Adding one-pion exchange term to the pionless potentials is done by a combining a pionless potential with the one-pion exchange potential through a CompoundPotential, its implementation shown in Listing 2.

Listing 2 Potentials can be combined, yielding a CompoundPotential. This is used to easily add a one-pion exchange term to other potentials.

```
struct CompoundPotential <: Potential
    V1::Potential
    V2::Potential
end

function(V::CompoundPotential)(r)
    V.V1(r) + V.V2(r)
end

function(V::CompoundPotential)(k, k′)
    V.V1(k, k′) + V.V2(k, k′)
end

+(V1::Potential, V2::Potential)::Potential = CompoundPotential(V1, V2)
```

Listing 3 Regularization is too a Potential wrapped around another Potential.

```
#= UV Regulatization =#
struct UVRegulator <: Potential
    V::Potential
    Λ::Float64  # Cutoff parameter [fm⁻¹]
end

function (V::UVRegulator)(k, k′)
    exp(-k^4/V.Λ^4) * V.V(k, k′) * exp(-k′^4/V.Λ^4)
end
```

Finally, a potential can be regularized with the smooth UV regulator [ref] by sandwiching a potential with the f_Λ factors, as implemented in Listing 3.

3.2 Minimization Procedure

Earlier works on the same topic[13, 12] often skimp on detailing the methods used to obtain the coefficients for the potentials. As a counterweight, the following is a detailed explanation of the minimization employed here. Modern works are of course much more detailed, but the methods they use are also too advanced to be employed here.

3.2.1 Region of Fit

Potentials derived from effective field theory are most accurate at low energies, i.e. the low infrared region. By construction, a fit here should give the best overall fit for all energies. However, the phase shift of the Reid potential is near linear for $E < 5$ MeV, before the peak. The more degrees of freedom a parameterized potential has, the more trouble minimization procedures will have in finding good coefficients that generalize without being able to see more features. It is therefore to expect that potentials with more degrees of freedom require data from higher and higher energies to perform a good fit.

Fitting to higher energies is undesirable as the EFT potentials quickly break down. In an effort to weight low energy points more, a bias is introduced using logarithmically spaced points to put more weight on points with low energy. We will examine the effect of fitting to different energy regions by changing the final energy E_{end} while holding Λ constant and examining the effect on the quality of the fit.

3.2.2 Fitting Error

Any form of fitting procedure require a measure of the error. A common measure is the square of the residuals, $(y_i - \text{fit}_i)^2$, used in least squares and χ^2 minimization. This is not necessarily optimal for our problem because the potentials derived from EFT are asymptotically good as $k \to 0$, and so one would expect the fit to get progressively worse as the energy increases. If the square of the residuals is used, the error at high energies will be weighted considerably more than the error at low energies, biasing the fit for a better "global" fit. A better choice might be to use the absolute error of the residuals $|y_i - \text{fit}_i|$ as suggested by Lepage[13], or the relative error $\frac{|y_i - \text{fit}_i|}{y_i}$. However, many standardized solvers rely on the properties of the square of the residuals to perform their minimization. We instead have to supply our own error function calculating the relative error and select a solver that tries to minimize this error.

This sends us to the problem of which minimization procedure to use. As we are using the Reid potential as the *Truth*, we need not care for empirical errors, only about obtaining a

good fit in a reasonable amount of time. This turns out to be substantially more difficult than what it seems at face value. There are two reasons for this. The first is that the dimension of the parameter space increases from 1 for LO to 4 with NNLO. Adding the pionic interaction adds another parameter. Not only does this make the solution space more shallow, it also introduces several local minima. Having obtained one solution, one can not set aside the fear that the solution is suboptimal, and many methods make it difficult to measure how much of the parameter space one has explored. Trials showed that gradient-based methods easily get stuck and several methods using exorbitant amount of time to obtain convergence. Simulated annealing found very good fits, but only after running for hours.

Another problem arises from the K-matrix method used to compute the phase shift. There is an inherent limitation to the method as the computation of δ perform an atan, setting an upper bound of $\pi/2$. Unfortunate values of the parameters or their combination leads to discontinuous jumps in the phase shift, which in turn causes the error to jump. The solvers I tried had difficulties dealing with this. The situation was improved by modifying the error function when noticing a jump in the phase shift to instead use

$$\Delta(\delta_{\text{reid}}, \delta) = |p \cdot \cot(\delta_{\text{reid}}(p)) - p \cdot \cot(\delta(p))|$$

as suggested by[16, 18]. This lifts the degeneracy in δ, but as it multiplied by the momentum p, larger momenta will weight considerably more. The intent is to steer the minimization procedure away from parameters causing jumps in a smooth fashion to prevent it from getting stuck.

3.2.3 Hyperparameters

Among the choices when performing the fit is how many points to include. Fig. 3.1 shows the relationship between the error in the fitting and number of points used for NLO, as well as the time usage. As for all fitting methods, using more points will reduce to error in the fit, but rather surprisingly the error increases rapidly when the number of points goes below ≈ 50. The reason seems to be the minimization struggling to achieve convergence. This is a bit worrying as Lepage[13, p. 35] used only 2 points, but no change I could come up with improved the situation.

The time usage is stochastic, tending to use more time when more points are used and when the number of fit parameters increase. The effect of number of points on the coefficients are shown in Fig. 3.2 along with bands showing the error relative to the coefficients from fitting with 200 points. The first coefficient is within 1% after 25 points, while the second requires 50 points to be within 10% of the best estimation. The ideal number of points seem to be about 50, but this causes NLO and NNLO to take an impractical amount of time to fit. As such, accuracy is sacrificed, and 10 points are used hereon unless otherwise states.

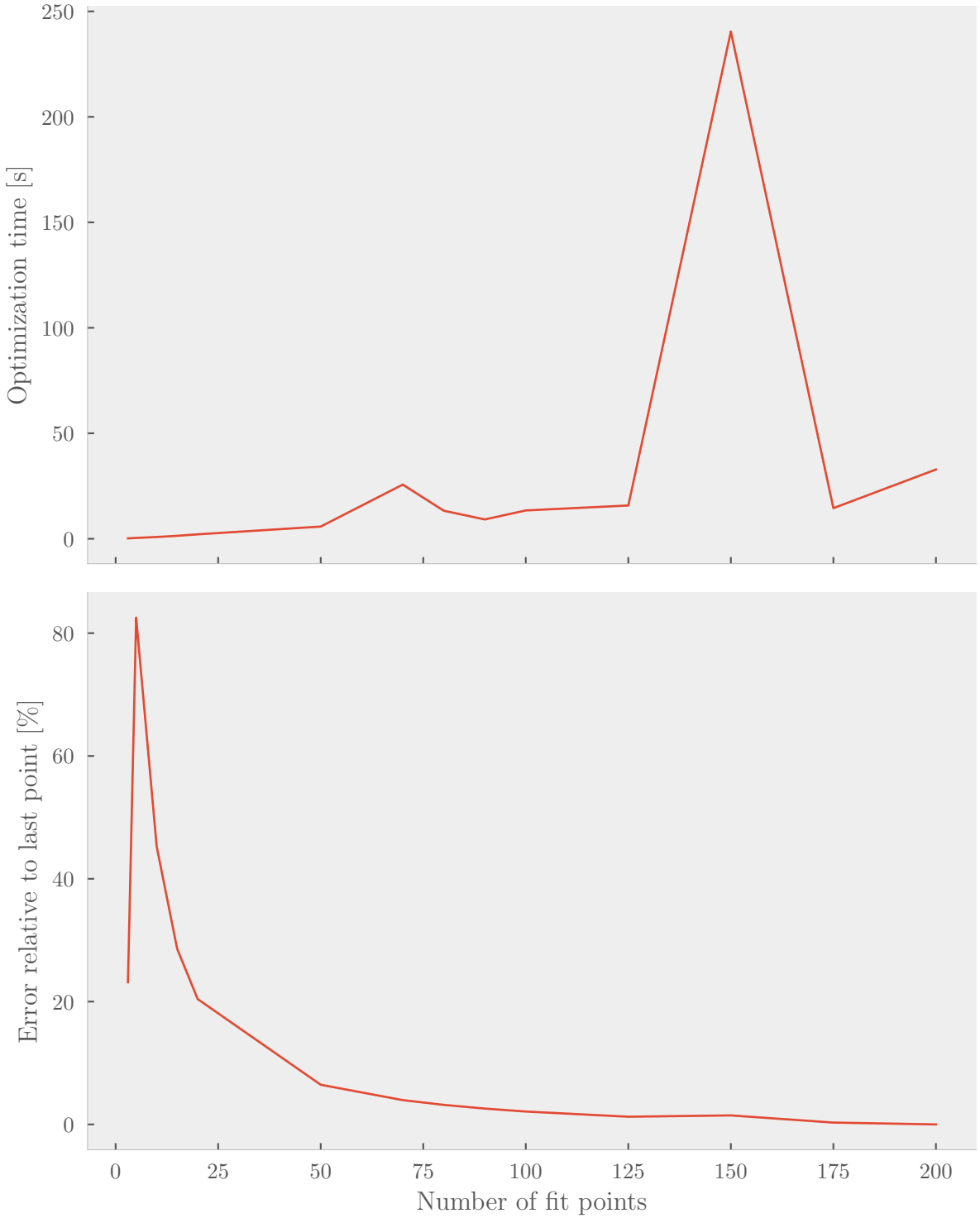

Figure 3.1: *The error (lower panel) in fitting NLO using a varying number of fitting points, as well as the time usage (top panel). The error is relative to the fitting from using 200 points. With* ≈ 50 *points the error is within* 10%*, and increasing the number of points yield only incremental improvement. The time usage is difficult to measure due to its stochastic nature. The top panel only shows an example which is rather unrepresentative. In general, the time increases significantly beyond* ≈ 20 *points, especially as the model complexity increases.*

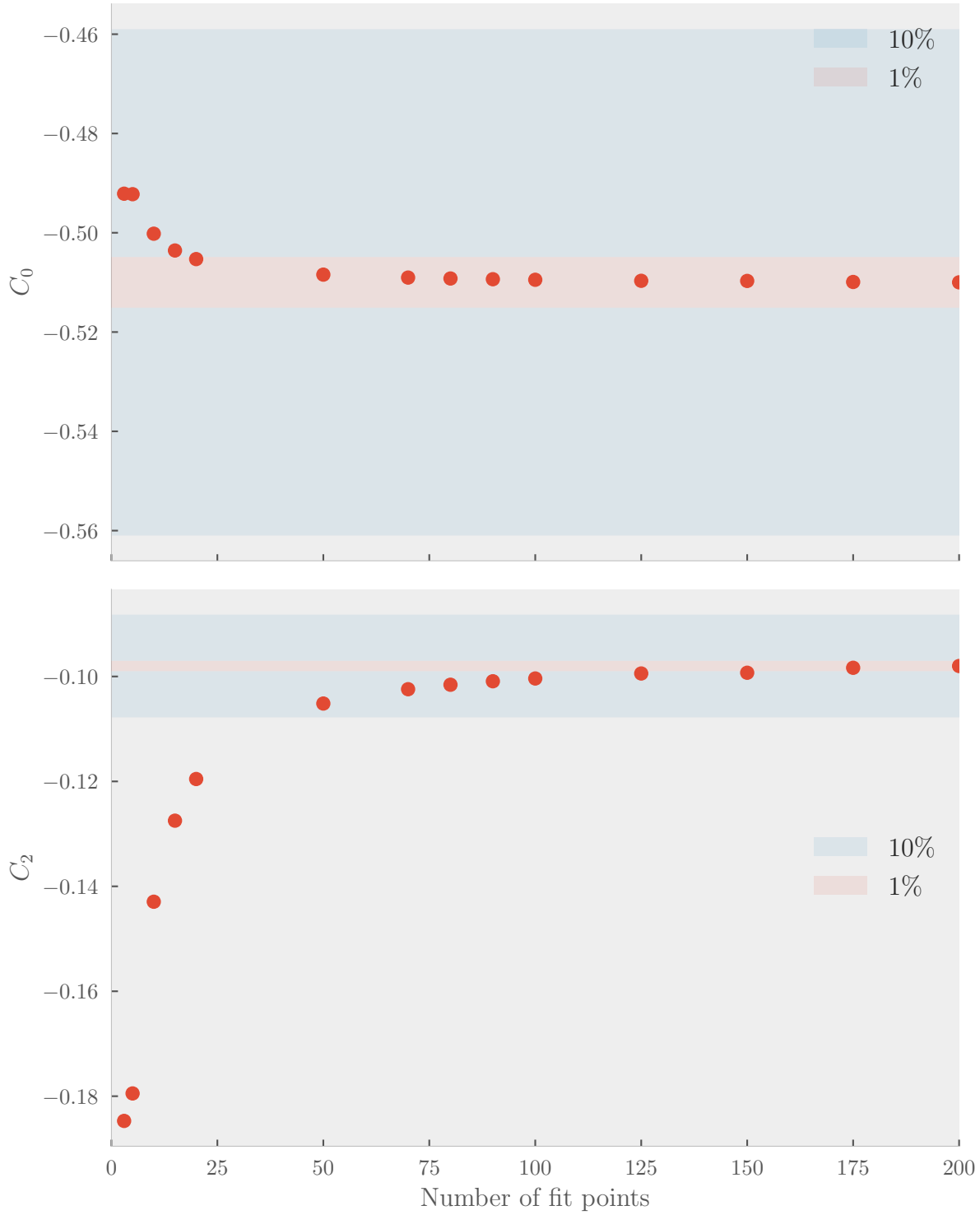

Figure 3.2: *The dependence of the coefficients on the number of points used in the fit. The bands show the error relative to the final result using* 200 *points. The points quickly converge as the number of points increase beyond* ≈ 50.

3.3 Finding Optimal Cutoff

The main goal is to find the optimal value of the cutoff parameter Λ for the different models. From the theory we expect that the models without a pion term will achieve their best result below $\Lambda = m_\pi$. Including a pion term will allow the models to account for simple pion exchange physics, and should be best at some value $\Lambda > m_\pi$. To explore whether this is borne out by calculations, the potentials are fitted with different values of Λ in the range 50 to ≈ 400 MeV.

When fitting the models, I had considerable difficulties with convergence. A tell-tale sign of convergence is that the parameters vary smoothly with Λ. To help the algorithm along, I extrapolated the model parameters from where it achieved convergence into the region where it had problems, squeezing the bounds as Λ increased. This worked well for LO and NLO, but only passably for NNLO.

3.4 Problems

The potentials are fitted to phase shifts generated by the Reid potential, but this introduces some subtle systematic errors. The Reid potential is a phenomenological NN potential composed of a sum of Yukawa interactions, not taking chiral or other symmetries into account. No matter how good its coefficients are fit to data, the potential can never achieve better accuracy than a sufficiently developed EFT potential. Reid (and later improvements) sought the best *gloabl* fit by minimizing χ^2 on the entire energy range, weighting by only the errors in the data. This neglects the fact that effective field theories scale with $(Q/\Lambda_\chi)^{\nu+1}$. When we use Reid to fit our EFT potential, it is therefore not to expect the errors we obtain to scale as nicely as it would have, had direct experimental observables been used instead.

4 Results and Discussion

4.1 Fit at Low Energies

The fit is expected to perform best at low energies. What is meant by "low" is arbitrary, usually taken lower than 1 MeV. To illustrate why this is ideal, we perform fits in three different regions, all starting at 10^{-3} MeV and stopping at 0.01, 1.0 and 100 MeV, respectively. Note that $\Lambda = m_\pi$, which we will see is suboptimal, but this does not change the point I will be trying to make. Fifty fit points are used in this section to exclude too few points as a source of error.

The resulting phase shift and relative error from fitting at low energies are shown in Fig. 4.1. Each order has less error than the previous in the fit region, and converging to the same error as the energy increases. However, the improvement from NLO to NNLO is completely negligible.

The two NNLO solutions illustrate a common problem with our method of fitting. A completely unconstrained fit, labeled simply "NNLO", give worse results than a constrained fit, labeled "NNLO Constrained", where the coefficients are forced to be within some hand picked regions. In general it is very difficult to fit the coefficients of NNLO, often requiring some bounds in order to keep the solver from getting stuck.

The values and 95% confidence intervals (CI) of each coefficient is given in Table 4.1. In particular, notice the small bounds on LO and NLO, indicating that the solver managed to find a stable solution.

	Coefficients			
Potential	C_0	C_2	C_4	C_4'
LO	-0.53			
NLO	-0.54	0.048		
NNLO	-0.50	0.054	-0.99	0.87
NNLO Constrained	-0.52	0.37	-1.18	-1.85

	95% Confidence Interval			
	C_0	C_2	C_4	C_4'
LO	2×10^{-6}			
NLO	1×10^{-5}	6×10^{-5}		
NNLO	3×10^{1}	7×10^{1}	6×10^{2}	1×10^{3}
NNLO Constrained	2×10^{1}	4×10^{1}	4×10^{2}	7×10^{2}

Table 4.1: *Coefficients found from fit at 10^{-3} to 10^{-1} MeV, as well as 95% confidence intervals of the coefficients. Only the rough magnitude is shown for the CI as the numbers change with each execution of the fit. [Labels refuse to align. Fix].*

4.1.1 Fit at Medium Energies

To see the effect of including higher energies, another fit was performed from 10^{-3} to 1 MeV. The resulting phase shifts and errors are shown in Fig. 4.2. There is a degradation everywhere except around 1 MeV when compared to the low energy fit. In particular, NLO is far worse, being negligibly better than LO. Another noteworthy change is the increasing

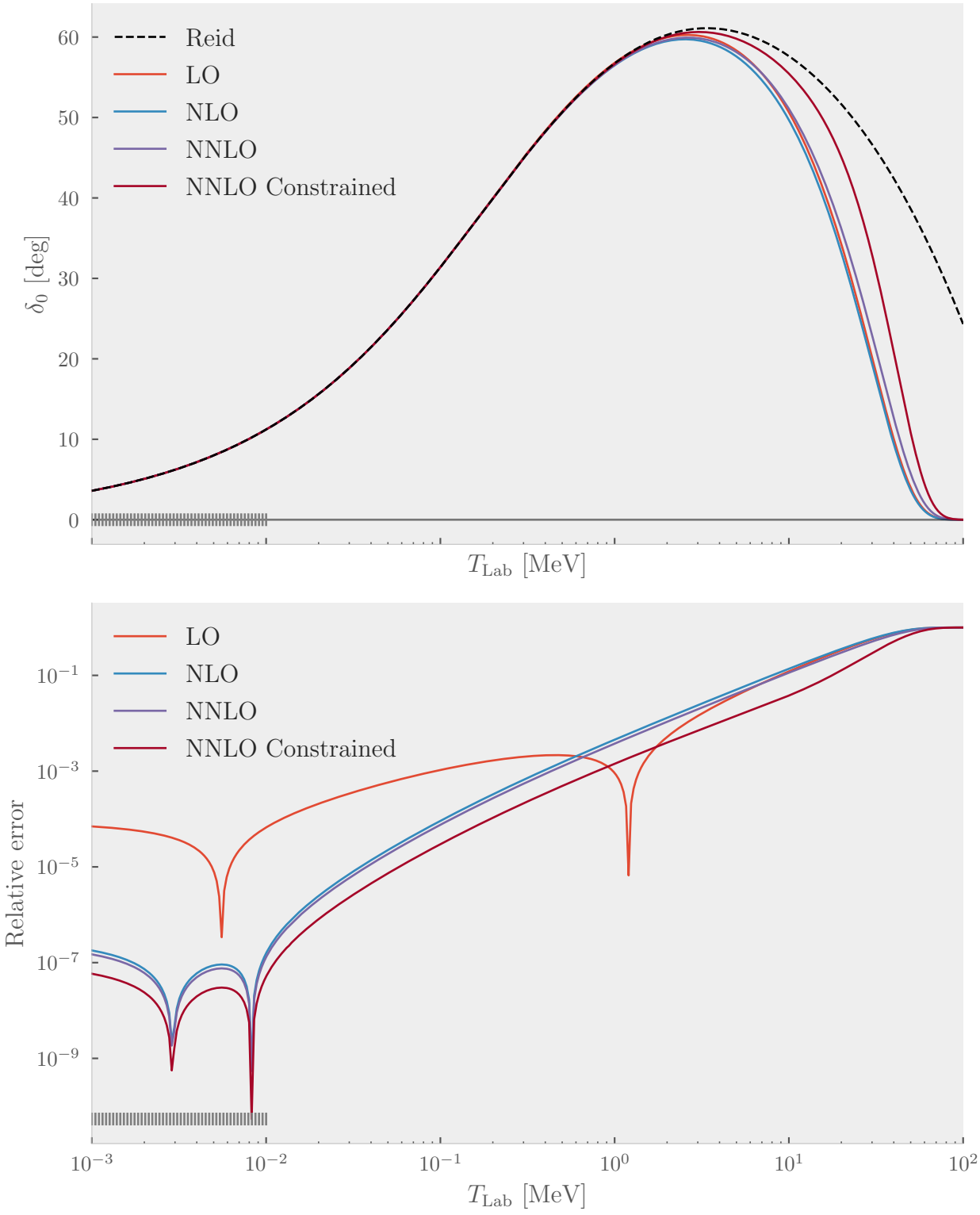

Figure 4.1: *Fit to low energy region with the phase shift shown in the top panel and relative error in the lower. The points used in the fit is indicated as ticks near the bottom of each plot. LO, NLO and NNLO had no limits to their coefficients, while NNLO Constrained was constrained to exclude "unphysical" phase shifts. The sharp dips are where the curves change sign.*

number of dips in the NNLO error, suggesting a more complex shape of the phase shift, as well as NNLO being better able to fit the Reid potential at energies higher than 1 MeV.

The coefficients and CI are shown in Table 4.2. The degradation in LO and NLO is reflected in the increased uncertainty of the coefficients by some orders of magnitude. The CIs of NLO are still small when compared to the value of the coefficient, indicating that the region used in the fit is worse than the lower energy. On the other hand, the NNLO has markedly smaller CIs, indicating that the higher energies are necessary for a good fit.

	Coefficients			
Potential	C_0	C_2	C_4	C_4'
LO	-0.53			
NLO	-0.53	0.015		
NNLO	-0.46	0.44	-2.4	-1.1

	95% Confidence Interval			
	C_0	C_2	C_4	C_4'
LO	1×10^{-5}			
NLO	1×10^{-3}	6×10^{-3}		
NNLO	4×10^{-1}	6×10^{-1}	5	1×10^{1}

Table 4.2: *Coefficients found from fit at 10^{-3} to 1 MeV, as well as 95% confidence intervals of the coefficients. Only the rough magnitude is shown for the CI as the numbers change with each execution of the fit.*

4.1.2 Fit at High Energies

Yet another fit was performed at energies 10^{-3} to 100 MeV, with results shown in Fig. 4.3, and yet again we see an increase in the relative error. All of the phase shift curves markedly deviate from the phase shift of the Reid potential. Of the three, NLO has the worst performance, while the simplest, LO, performs the best.

Table 4.3 gives the CIs of the coefficients. The same tale repeats, with CI becoming increasingly wide. The CIs of the coefficients of NNLO are utterly useless, spanning six and eight orders of magnitude, illustrating that the least squares method fails to converge to a good set of coefficients.

4.1.3 Dependence on Fit Region

The previous three subsections showed the consequence of fitting LO, NLO and NNLO to different energies. LO is consistently well behaved, with fast convergence for the minimization procedures and small dependence on the hyperparameters. Of course, the reason for this is its simplicity, with a small parameter space and few parameters that give nonsensical results. For all of the potentials, the error in the region of fit is lowest for $E_{\text{end}} = 1 \times 10^{-2}$ MeV, but more importantly, the *slope* of the error is the same. To stress this point, the NLO potential is fitted at a range of different energies E_{end} from 1×10^{-2} to 100 MeV, see Fig. 4.4. Two features are obvious. Firstly, a smaller region of fit will always give a smaller fit error, simply because it is easier to find arbitrarily good solutions to homogeneous data. Secondly, the slope above the fit region remains the same up to about 5 MeV. Thus, we will get fairly

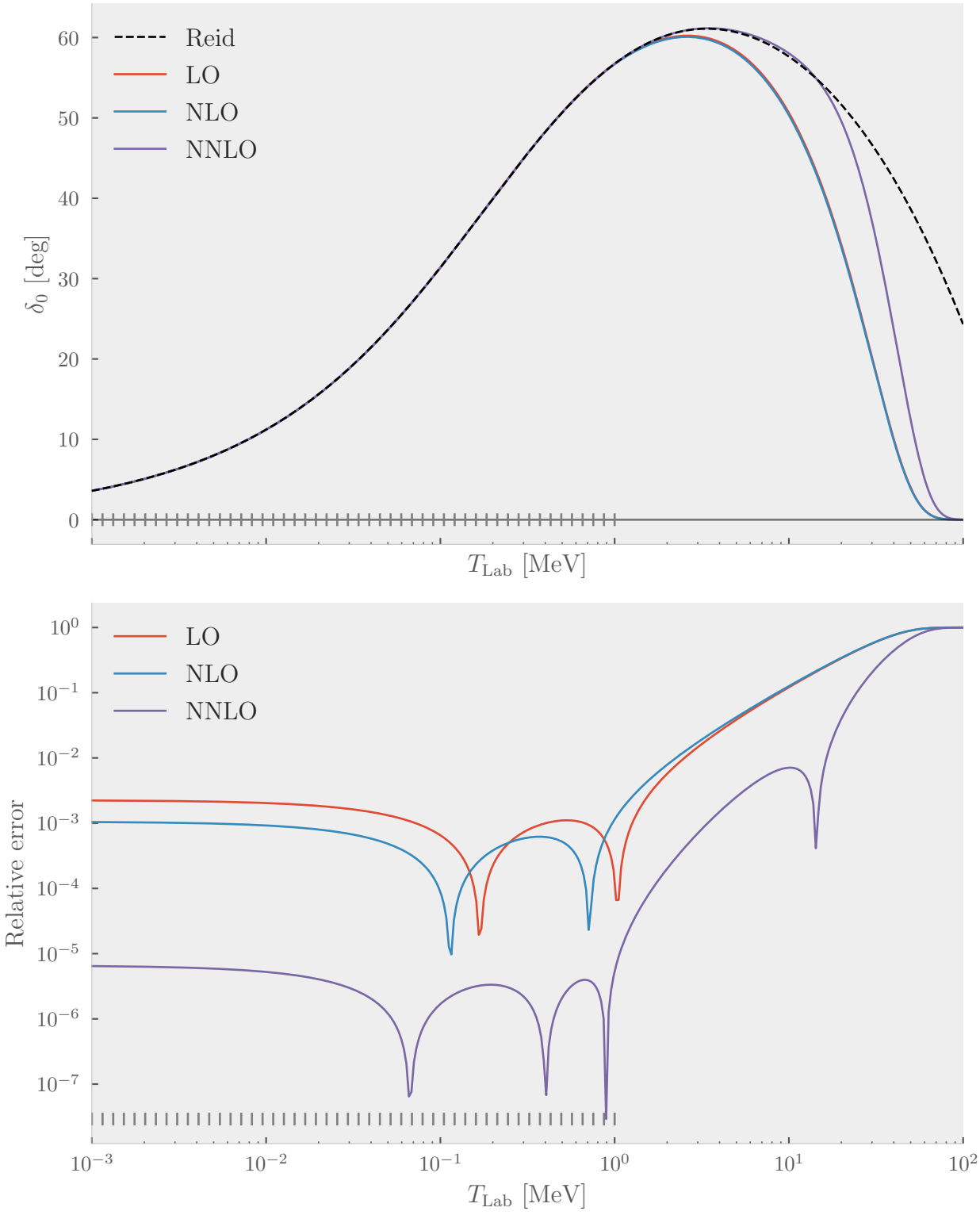

Figure 4.2: *Fit to the mid energy region with the phase shift shown in the top panel and relative error in the lower. The points used in the fit are indicated as ticks near the bottom of each plot. No constraints were used on the coefficients. When compared to the low energy fit, all perform worse in low energy region. NLO does negligibly better than LO.*

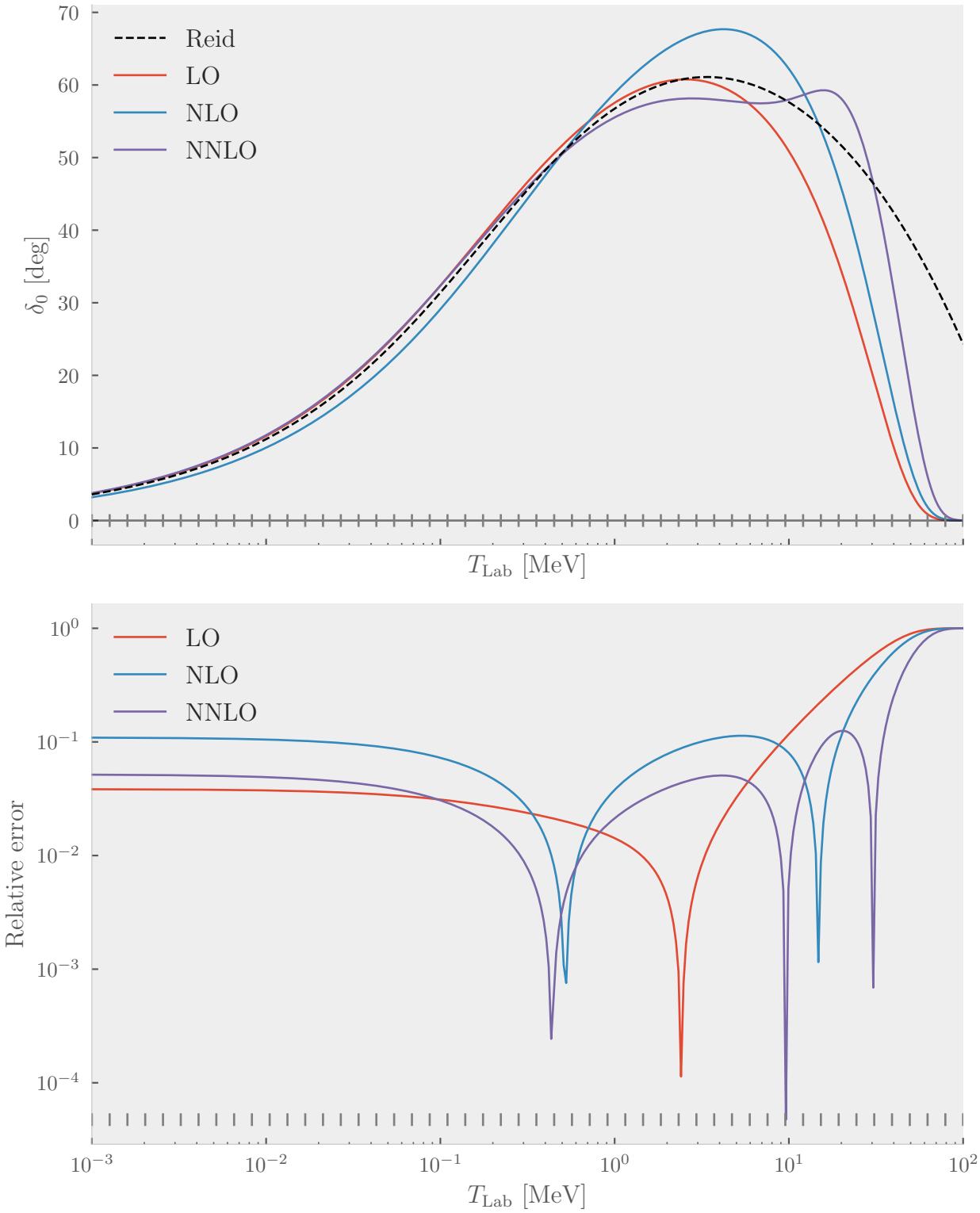

Figure 4.3: *Fit to the high energy region with the phase shift shown in the top panel and relative error in the lower. The points used in the fit are indicated as ticks near the bottom of each plot. The errors are several order of magnitude greater when compared to Fig. 4.1 and Fig. 4.2*

	Coefficients			
Potential	C_0	C_2	C_4	C_4'
LO	-0.53			
NLO	-0.40	-0.58		
NNLO	-0.70	1.3	-3.0	-9.6

	95% Confidence Interval ($\pm$)			
	C_0	C_2	C_4	C_4'
LO	3×10^{-2}			
NLO	1×10^{-1}	6×10^{-1}		
NNLO	2×10^{6}	3×10^{6}	1×10^{8}	1×10^{8}

Table 4.3: *Coefficients found from fit at 10^{-3} to 100 MeV, as well as 95% confidence intervals of the coefficients. Only the rough magnitude is shown for the CI as the numbers change with each execution of the fit. [Labels refuse to align. Fix].*

similar results if we use regions below 5 MeV, in line with the common rule of thumb of fitting to the most infrared region possible.

The figure also highlights that what we mean by "error" depends on the region of interest. If we are only concerned about low energy physics, then we gain nothing by fitting at higher energies. If we instead would like an okay description at a wide range of energies, then perhaps including higher energies in the fit will yield better results. The black line shows the solution with the lowest total error in the range 10^{-3} to 100 MeV, suggesting that using energies up to 10 MeV can be beneficial. In order to be as consistent with the method of Lepage as possible, energies from 10^{-3} to 0.1 MeV is used from here on.

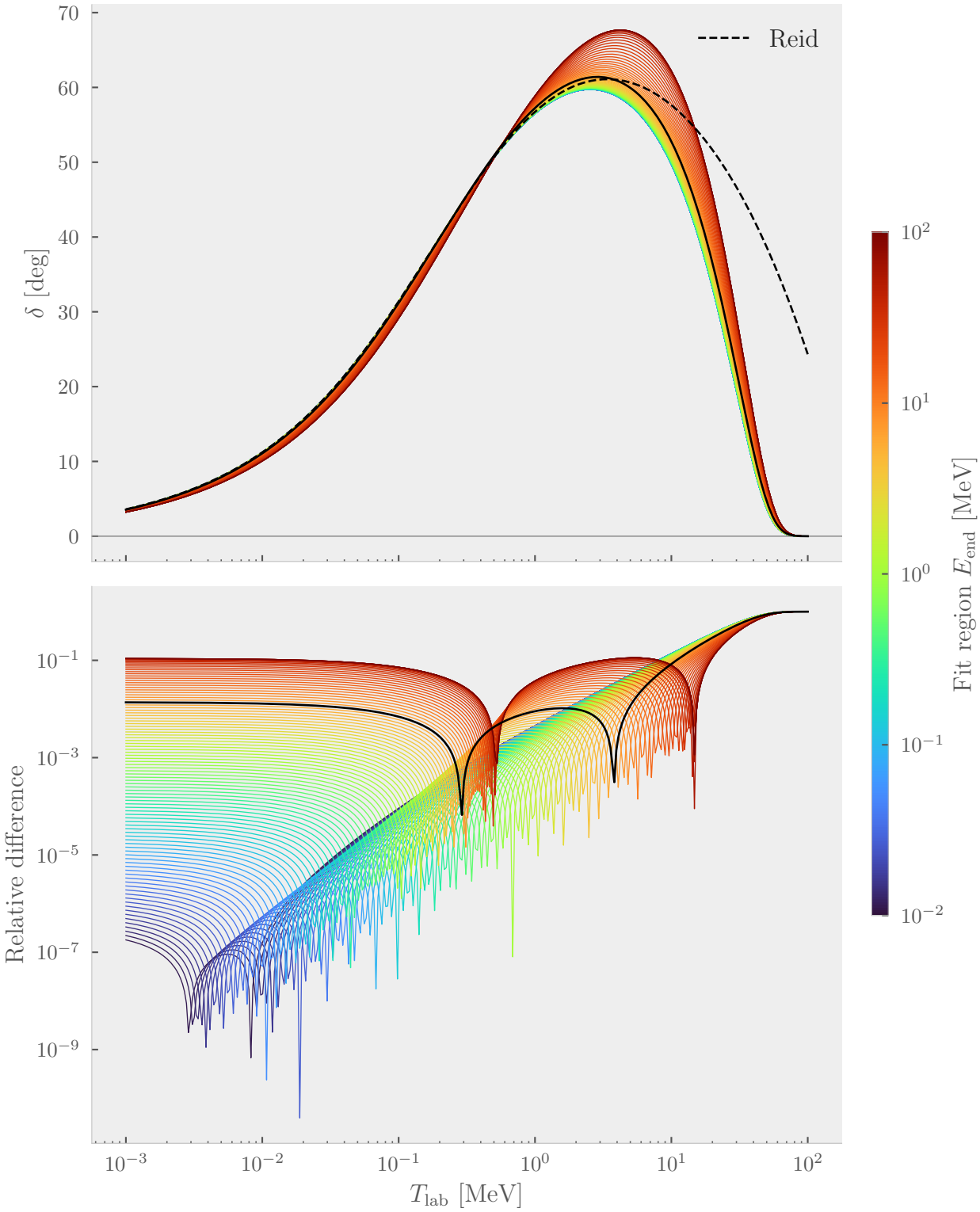

Figure 4.4: *(Top) The phase shift from NLO and (bottom) the relative error. The potential was fit in the region* $[10^{-3}, E_{\text{end}}]$ *MeV to illustrate how the fit region affects the result. The black line shows the solution with the lowest total error in the range* 10^{-3} *to 100 MeV.*

4.2 Dependence on Λ

For each model the cutoff parameter Λ was varied from 50 to 600 MeV, and the models were fitted in the region $[10^{-3}, 10^{-1}]$ MeV with 10 points. The results are summarized in figures Figs. 4.5 and 4.6. The best values of Λ are given in Table 4.4 and coefficients in Table 4.5.

The pure 1π toy term is a good model when only looking at very low energies. This is of course expected, as it is precisely the long range interaction that the pionic terms model. Nor is it surprising that the 1π term does not vary significantly with the value of Λ. It does not model any short range physics, so no higher diagrams are being cut off nor introduced that could change the value.

The other models show several systematic behaviors. Increasing the order of the model decreases the error both in the region of fit and above. Adding 1π too decreases the error, as well as systematically increasing the cutoff Λ. LO is particularly nice in this regard, obtaining its minimum right before m_π and failing miserably after, while LO $+ \pi$ obtains its minimum above m_π and improves the fit by two orders of magnitude[6].

Both LO and NLO break down when $\Lambda > m_\pi$, but surprisingly NLO carries on its merry way far beyond. NNLO, on the other hand, fails long before $\Lambda = m_\pi$. Adding 1π improves all models, with NLO$+\pi$ and NNLO$+\pi$ obtaining their minimum at approximately at $\Lambda \approx 270$ MeV. That they break down at the same value alludes to higher energy physics being involved, perhaps due to the toy nature of our 1π term, or our exclusion of 2π and higher order terms. Another possibility is that perhaps quarks can be resolved near this energy, dooming EFT to become inaccurate.

Since we are following the approach of Lepage, it is natural to compare our results. See figures 6 to 8 in [13]. Our methods and data are not identical, but some general remarks can be made. The slopes in Lepage's errors exhibit the typical power counting behavior, with each additional order increasing the log-log slope by approximately T_{lab}^{+2}. Our models do not show this. In fact, each order $\pm 1\pi$ has nearly identical error, up to a shift. I do not have any explanation for why this is the case, except for a failure of the minimization.

However, there is a systematic improvement when adding the 1π term. The term increases the slope of each model by precisely T_{lab}^{+2}. This runs counter to Lepage's assertion that "Evidently one-pion exchange contributes little to the phase shift at most energies" [13, p. 36]. I hazard to guess that the reason for the discrepancy is that the contribution of a term can not be determined by fitting the term by itself. The different terms capture different physical aspects, so fitting an "incomplete" model forces it to account for as many aspects as possible. In particular, fitting the contact terms by themselves makes them also fit the long range, low energy data, something they were never constructed to model. Adding the 1π term alleviates this issue, greatly improving the overall fit. It is perhaps more constructive to compare the coefficients of the models, as in Table 4.5. When the 1π term is added, the coefficients of each order more or less align, with each order term having a lower coefficient[7]. This constrats to the pionless models where the coefficients vary more, and the order of the coefficients are about the same for each term.

[6] Averaged over 1×10^{-3} to 100 MeV. The improvement is a whopping 4 orders of magnitude in the region of fit.

[7] Both C_4 and C_4' correspond to terms of order p^4. The fact that they are of different sign suggest some cancelation is going on, perhaps due to poor fit.

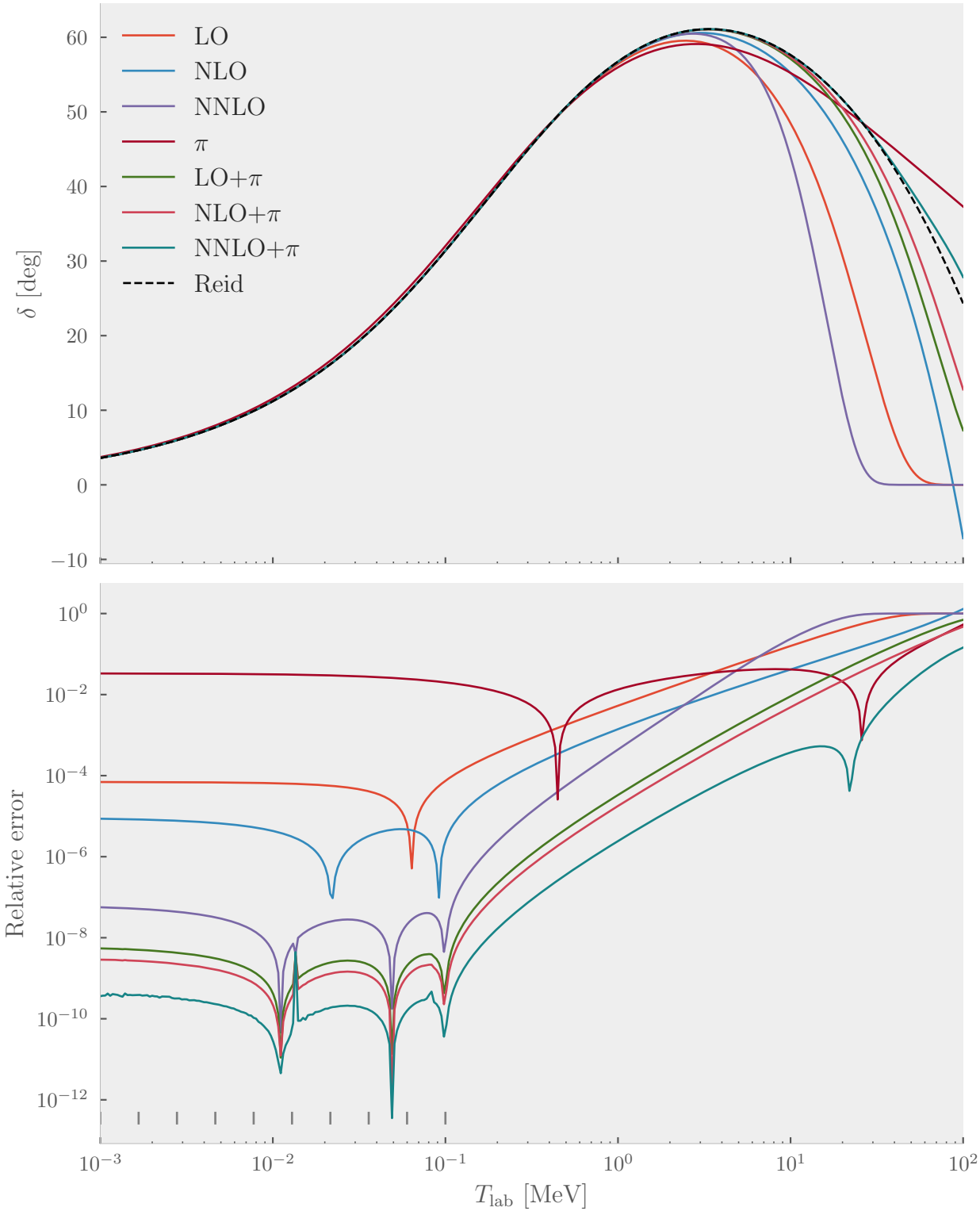

Figure 4.5: *(Top) The* $^1S_0$ *phase shift calculated from each ChEFT potential using their optimal value of* Λ*, along with the "true" Reid68 potential.* π *denotes the pure* 1π *toy term. (Bottom) the relative error in the aforementioned phase shift. The 10 dashes at the bottom mark the points used in the fit. All dips are figments of where the absolute value changes sign.*

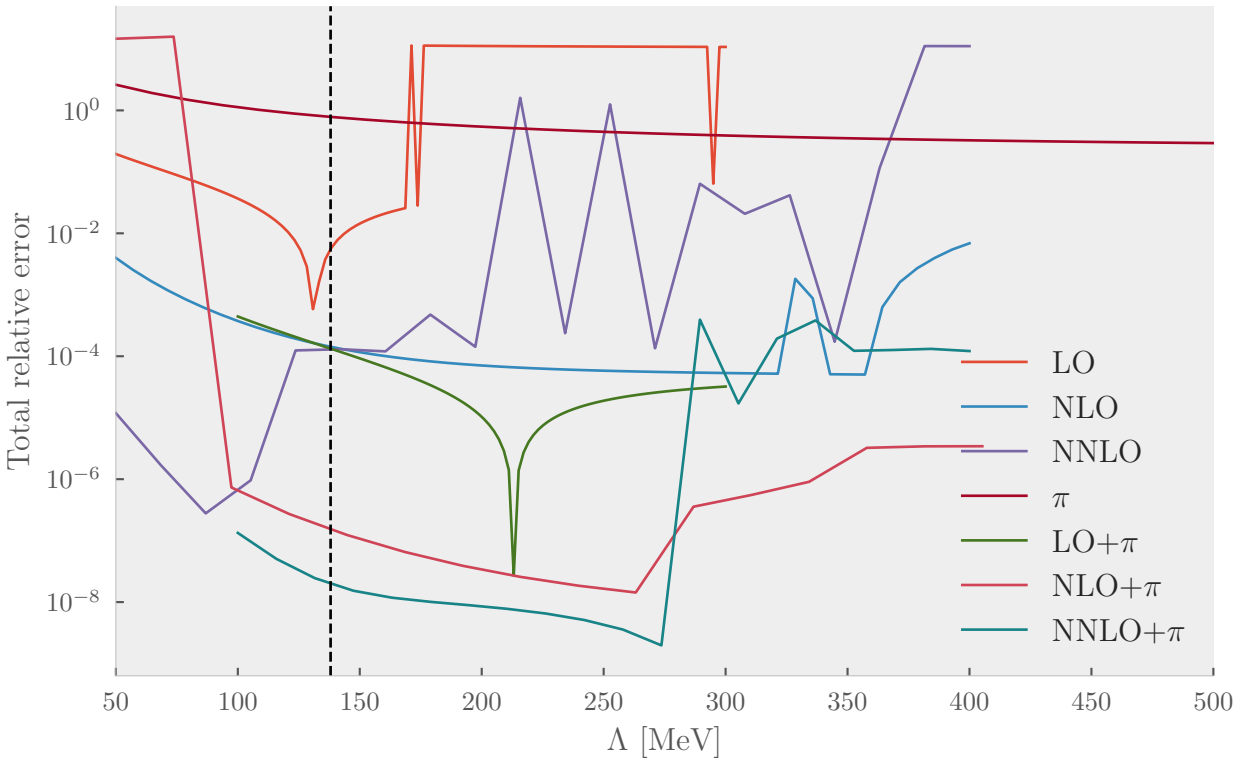

Figure 4.6: *The relative error of the* $^1S_0$ *phase shift summed in the region of fit,* 1×10^{-3} *to* 1×10^{-1} *MeV. It is plotted against* Λ *as it runs through* ≈ 50 *to* ≈ 400 *MeV.* $\Lambda = m_\pi$ *is shown as a dashed black line. The pionless potentials with the exception of NLO reach their minima below* m_π*, while the inclusion of the* 1π *toy term raise the minima to about 270 MeV. The pure pion term never achieves a minimum.*

Model	Λ [MeV]
LO	132
NLO	357
NNLO	86
π	>1500
LO+π	213
NLO+π	263
NNLO+π	273

Table 4.4: *The best values of* Λ *for each model. No uncertainties are given as no sensible measure could be derived.*

Model	C_0	C_2	C_4	C_4'	C_π
LO	-5.55×10^{-1}				
NLO	-3.92×10^{-1}	2.48×10^{-1}			
NNLO	-6.51×10^{-1}	4.59×10^{-1}	-1.53×10^{1}	-1.59×10^{1}	
π					-1.57×10^{-1}
LO+π	-2.23×10^{-1}				-7.82×10^{-2}
NLO+π	-2.33×10^{-1}	5.43×10^{-2}			-6.62×10^{-2}
NNLO+π	-2.00×10^{-1}	8.68×10^{-2}	-9.50×10^{-2}	4.53×10^{-2}	-5.67×10^{-2}

Table 4.5: *The coefficients of each model. The pionic models have similar coefficients, while the non-pionic show more variance. Note also the high coefficients for the p^4 terms of NNLO, suggesting that the minimization failed to find reasonable values. No uncertainties are given as no reasonable measure could be found for all of the models, in particular NNLO$\pm\pi$, but for most models the minimization converged to several decimal places.*

A possible interjection is that the breakdowns we see are not due to too high energy physics cropping up, but simply an unfortunate consequence of our fitting procedure. To justify why this is not the case, we can look at how the parameter changes as Λ increases. Fig. 4.7 shows the parameters of NLO+π as Λ changes. All of the parameters converge, yet the error keeps on increasing beyond $\Lambda = 263$ MeV. The same convergence is seen when the bounds on the parameters are removed, although less smooth, hence the bounds can not be at fault. Although we may have gotten stuck in local minima, the breakdowns we see are likely "true" breakdowns. By the same reasoning, we can guess that the minimization of NNLO failed as the parameters show no sign of convergence, while NNLO+π managed to achieve convergence.

When the minimization was run several times, all models consistently broke down at around the same values of Λ, giving credence that the optimal values are not flukes. However, as the number of parameters increase, the minimization gets increasingly sensitive to initial conditions. For NNLO, another minimum was found for $\Lambda = 230$ MeV, but as this solution had three order of magnitude larger error, it was ignored. Nevertheless, it illustrates the problem of multiple minima.

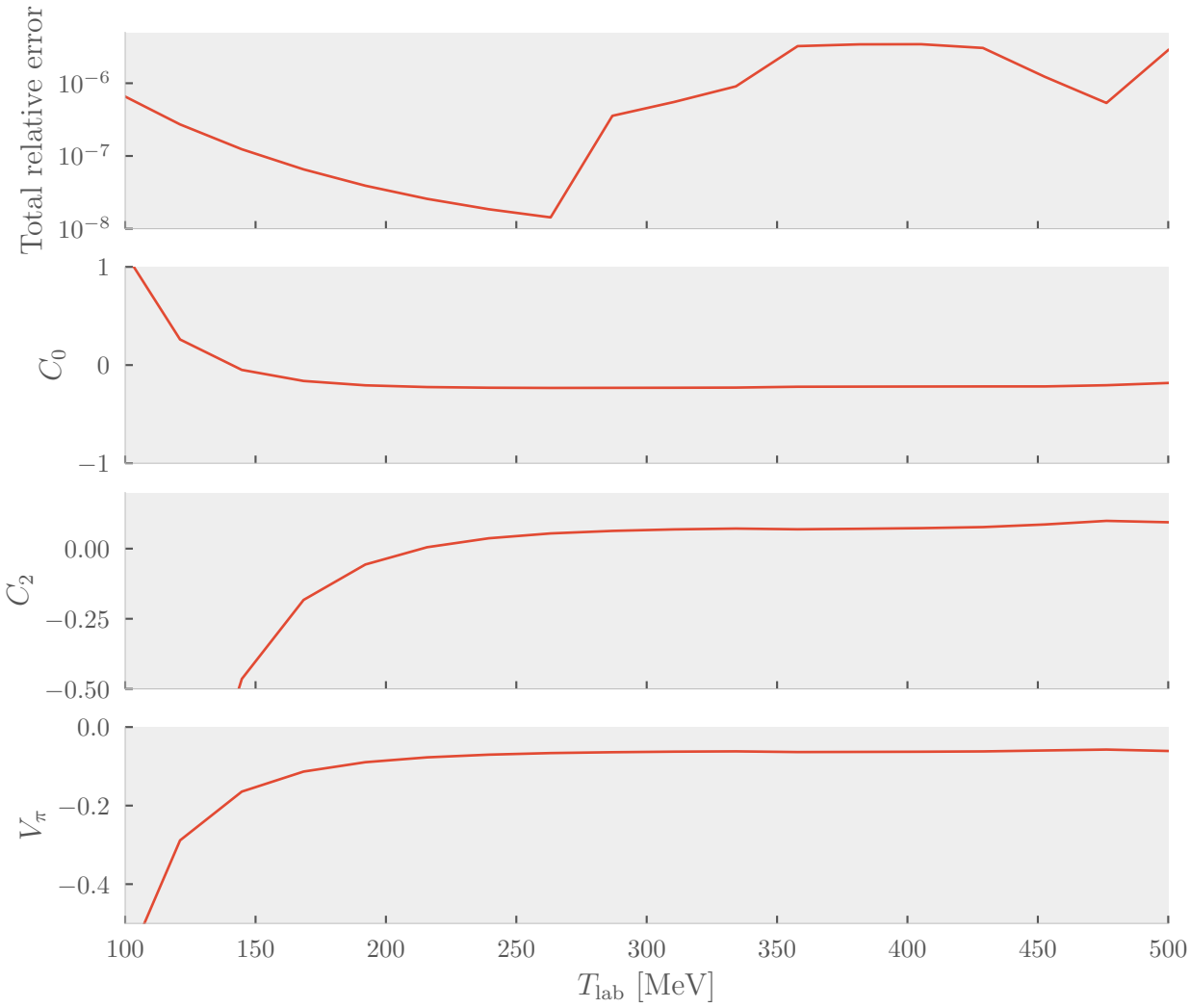

Figure 4.7: *The coefficients of NLO+π and fit error as a function of Λ. When $\Lambda > 200$ MeV, the coefficients converge while the error keeps decreasing. After the optimal lambda, the error quickly increases, even when the coefficients remain near constant.*

4.3 Search for Power-Law Improvement

Increasing the chiral order has lead to better models, but the expected power law improvement has remained missing. I do not know why this is, but suspect it is mainly due to poor minimization. Fig. 4.5 suggests that the different potentials achieve convergence at different values of Λ. In other words, comparing the results for a specific Λ can lead to a mediocre fit for some of the potentials, destroying any power law improvement that would have been present.

A possible solution is to fit the models for different values of Λ and find a set of curves that exhibit a power law improvement. The best results are shown in Fig. 4.8 and Fig. 4.9, using values $\Lambda = 100$ MeV and $\Lambda = 150$ MeV, respectively. The pionless models exhibit a power-law improvement, with the difference of the exponents being $0 : 0.7 : 1.6$. The improvement from NLO to NNLO is the closest to a $+2$ improvement. The pionic models has a significantly weaker improvement with $0 : 0.98 : 0.1$.

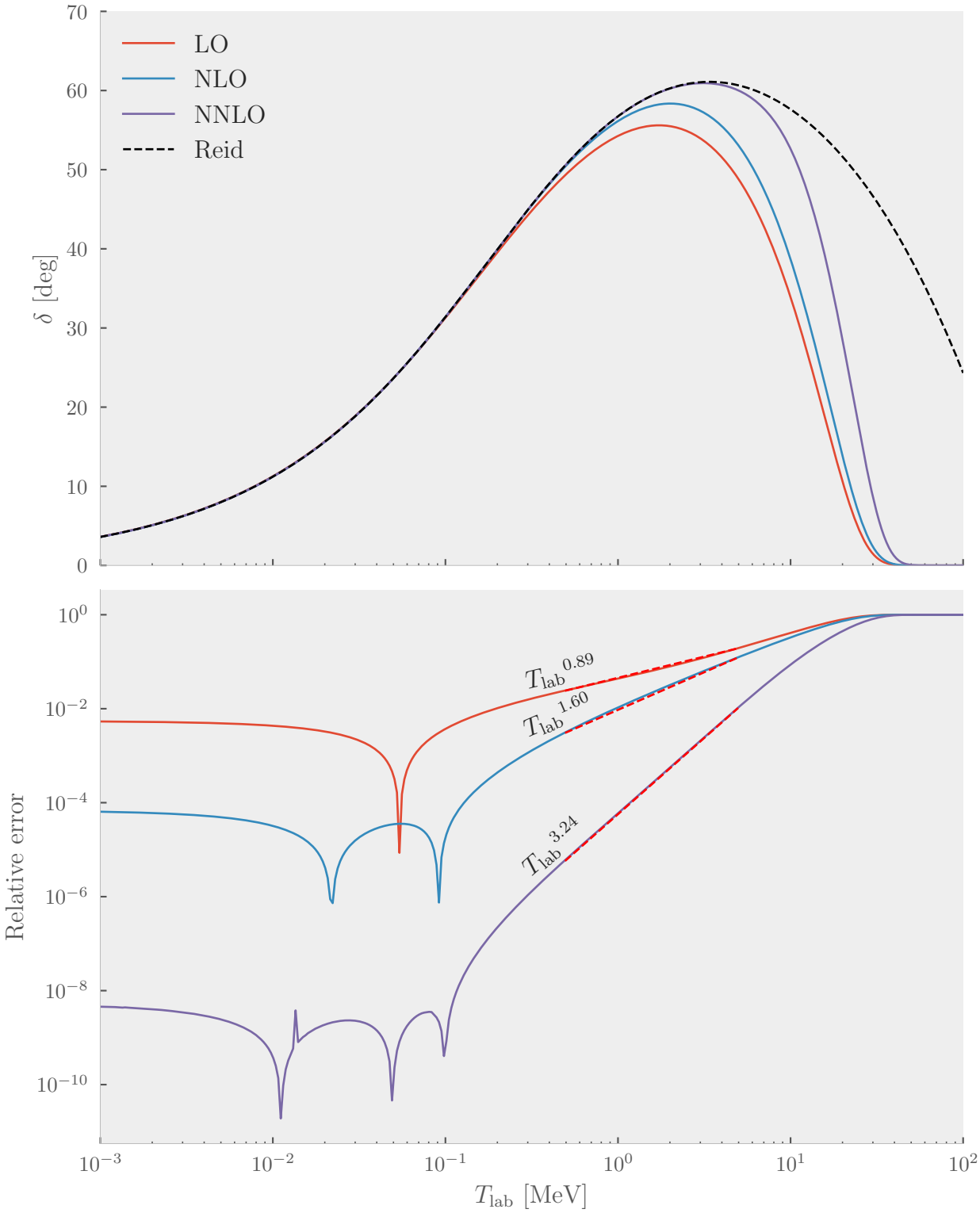

Figure 4.8: *The phase shift (top) and error in phase shift using pionless models. A best fit log-log line is shown from about* 0.5 *to 10 MeV, along with the exponent. The cutoff was* 100 *MeV.*

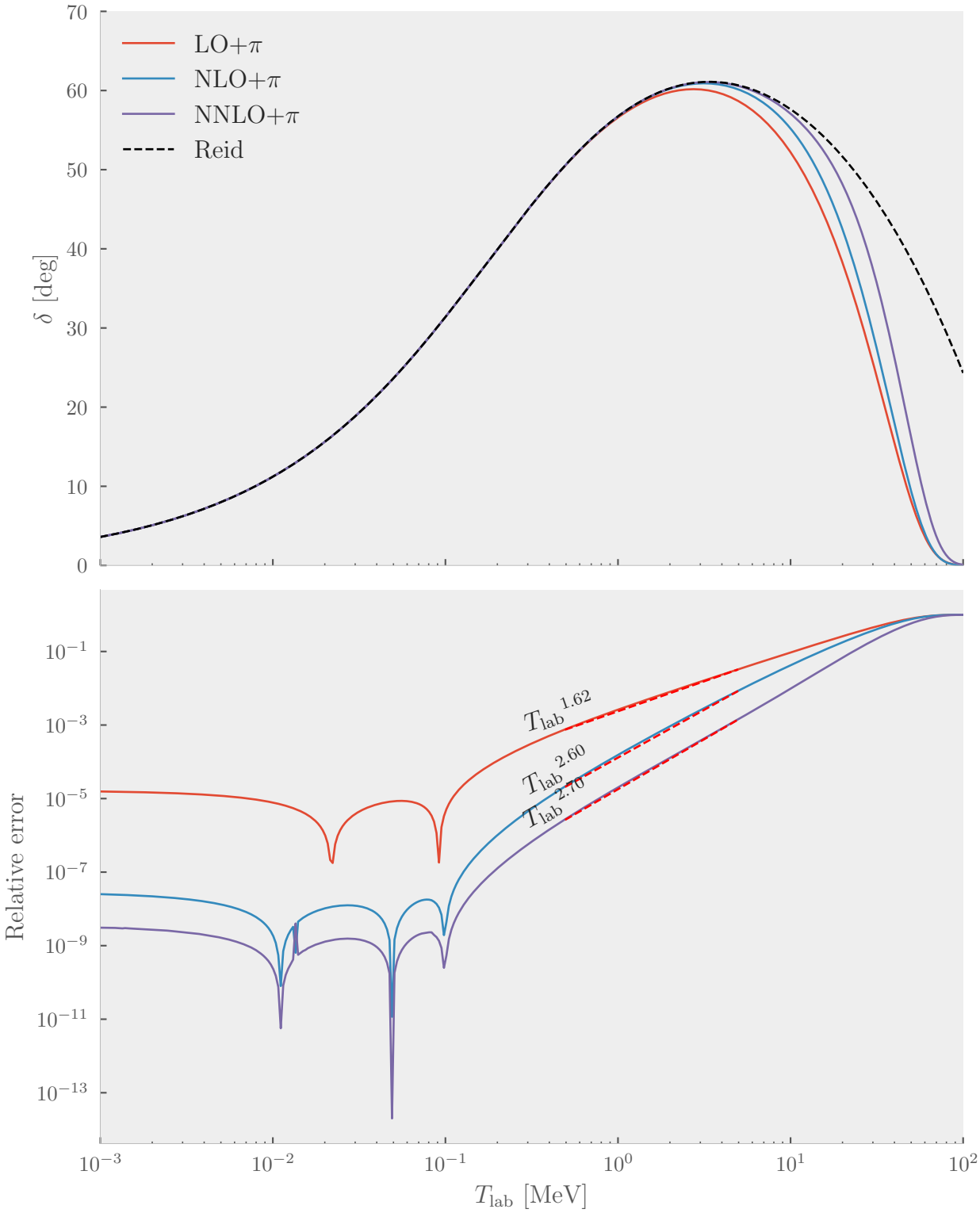

Figure 4.9: *The phase shift (top) and error in phase shift using models with* 1π *term. A best fit log-log line is shown from about* 0.5 *to 10 MeV, along with the exponent. The cutoff was* 150 *MeV.*

5 Conclusion

A basic overview of chiral perturbation theory was presented, casting low energy nuclear physics as the low energy limit of QCD. Unlike pre-QCD and phenomenological models, ChPT provides a rigorous treatment of the error, allowing for systematic improvement. Its faults lie in its construction, being only valid at low energies.

Several toy potentials inspired by effective field theory were constructed and used to model np-scattering of ${}^1S_0$ partial waves. They were fitted to low energy phase shifts generated by the traditional Reid potential, and compared to phase shifts at higher energies. The fitting procedure was fraught with problems, both theoretical and practical, having difficulties in obtaining good fits and convergence. The results showed consistent yet marginal improvement as higher order terms were added, not in line with the improvement expected from power counting arguments, and in disagreement with the results of Lepage. Poor fitting and too simplistic models were suggested as causes, but none were satisfying in explaining the disagreement.

EFT models involving a pionic term is expected to perform better than pionless, and this was borne out by the calculations. Pionless models gave best results right below $\Lambda = m_\pi$, while the inclusion of the 1π toy term yielded best result near $\Lambda = 270$ MeV, in agreement with Lepage.

References

[1] CERN Courier. *DISCOVERY OF THE PION — 1947*. 1997. URL: http://fafnir.phyast.pitt.edu/particles/pion.html (visited on 01/05/2021) (cit. on p. 1).

[2] Hideki YUKAWA. "On the Interaction of Elementary Particles. I". In: *Proceedings of the Physico-Mathematical Society of Japan. 3rd Series* 17 (1935), pp. 48–57. DOI: 10.11429/ppmsj1919.17.0_48 (cit. on p. 1).

[3] C. M. G. LATTES, G. P. S. OCCHIALINIDR., and C. F. POWELLDR. "Observations on the Tracks of Slow Mesons in Photographic Emulsions*". In: *Nature* 160.4066 (Oct. 1947), pp. 453–456. ISSN: 1476-4687. DOI: 10.1038/160453a0. URL: https://doi.org/10.1038/160453a0 (cit. on p. 1).

[4] A. R. Erwin et al. "Evidence for a $\pi - \pi$ Resonance in the $I = 1$, $J = 1$ State". In: *Phys. Rev. Lett.* 6 (11 June 1961), pp. 628–630. DOI: 10.1103/PhysRevLett.6.628. URL: https://link.aps.org/doi/10.1103/PhysRevLett.6.628 (cit. on p. 1).

[5] Junji Iwadare et al. "Two-Nucleon Problem with Pion Theoretical Potential, III: p-p Scattering at 18.2 Mev". In: *Progress of Theoretical Physics* 16.6 (Dec. 1956), pp. 604–612. ISSN: 0033-068X. DOI: 10.1143/PTP.16.604. eprint: https://academic.oup.com/ptp/article-pdf/16/6/604/5384206/16-6-604.pdf. URL: https://doi.org/10.1143/PTP.16.604 (cit. on p. 1).

[6] R. Machleidt, K. Holinde, and Ch. Elster. "The bonn meson-exchange model for the nucleon—nucleon interaction". In: *Physics Reports* 149.1 (1987), pp. 1–89. ISSN: 0370-1573. DOI: https://doi.org/10.1016/S0370-1573(87)80002-9. URL: https://www.sciencedirect.com/science/article/pii/S0370157387800029 (cit. on pp. 1, 4).

[7] A.D. Jackson, D.O. Riska, and B. Verwest. "Meson exchange model for the nucleon-nucleon interaction". In: *Nuclear Physics A* 249.3 (1975), pp. 397–444. ISSN: 0375-9474. DOI: https://doi.org/10.1016/0375-9474(75)90666-1. URL: https://www.sciencedirect.com/science/article/pii/0375947475906661 (cit. on p. 1).

[8] M. Lacombe et al. "Parametrization of the Paris $N - N$ potential". In: *Phys. Rev. C* 21 (3 Mar. 1980), pp. 861–873. DOI: 10.1103/PhysRevC.21.861. URL: https://link.aps.org/doi/10.1103/PhysRevC.21.861 (cit. on pp. 1, 4).

[9] S. Weinberg. "Phenomenological Lagrangians". In: *Physica A* 96.1-2 (1979), pp. 327–340. ISSN: 0378-4371. URL: http://inis.iaea.org/search/search.aspx?orig_q=RN:11507205 (cit. on p. 3).

[10] E. Epelbaum. "Nuclear forces from chiral effective field theory". In: *Progress in Particle and Nuclear Physics* 67.2 (2012). From Quarks and Gluons to Hadrons and Nuclei, pp. 343–347. ISSN: 0146-6410. DOI: https://doi.org/10.1016/j.ppnp.2011.12.041. URL: https://www.sciencedirect.com/science/article/pii/S014664101100158X (cit. on pp. 3, 6).

[11] Steven Weinberg. "Effective chiral lagrangians for nucleon-pion interactions and nuclear forces". In: *Nuclear Physics B* 363.1 (1991), pp. 3–18. ISSN: 0550-3213. DOI: https://doi.org/10.1016/0550-3213(91)90231-L. URL: https://www.sciencedirect.com/science/article/pii/055032139190231L (cit. on p. 3).

[12] R. Machleidt and D.R. Entem. "Chiral effective field theory and nuclear forces". In: *Physics Reports* 503.1 (2011), pp. 1–75. ISSN: 0370-1573. DOI: https://doi.org/10.1016/j.physrep.2011.02.001. URL: https://www.sciencedirect.com/science/article/pii/S0370157311000457 (cit. on pp. 3, 9).

[13] Peter Lepage. *How to Renormalize the Schrodinger Equation*. 1997. arXiv: nucl-th/9706029 [nucl-th] (cit. on pp. 3, 5–7, 9, 10, 21).

[14] Willem Hendrik Dickhoff and Dimitri VY Van Neck. *Many-body theory exposed! Propagator description of quantum mechanics in many-body systems*. World Scientific Publishing Company, 2008 (cit. on p. 3).

[15] R. Machleidt and D.R. Entem. "Chiral effective field theory and nuclear forces". In: *Physics Reports* 503.1 (June 2011), pp. 1–75. ISSN: 0370-1573. DOI: 10.1016/j.physrep.2011.02.001. URL: http://dx.doi.org/10.1016/j.physrep.2011.02.001 (cit. on p. 4).

[16] James V Steele and RJ Furnstahl. "Regularization methods for nucleon-nucleon effective field theory". In: *Nuclear Physics A* 637.1 (1998), pp. 46–62 (cit. on pp. 6, 10).

[17] Roderick V Reid. "Local phenomenological nucleon-nucleon potentials". In: *Annals of Physics* 50.3 (1968), pp. 411–448. ISSN: 0003-4916. DOI: https://doi.org/10.1016/0003-4916(68)90126-7. URL: http://www.sciencedirect.com/science/article/pii/0003491668901267 (cit. on p. 6).

[18] R. John Taylor. *Scattering Theory*. John Wiley & Sons, Inc., 1972 (cit. on p. 10).